

Fig. 1. The cyclic I - E curve of the pyrrole monomer's polymerizing reaction and oxidation, reduction reaction. Electrolyte solution: 0.1 M $\text{LiClO}_4 + \text{CH}_3\text{CN}$; scanning rate: 20 mV s^{-1} .

the potential range of -700 to $+1000$ mV. In the oxidation curve 1, there was no reactive current as the oxidation potential increased from -700 to $+650$ mV. This is because when the oxidation potential is lower than $+650$ mV, the pyrrole monomers cannot be oxidized into cations. Dimer or oligomer was unable to form, so there was no transfer of electrons. When the oxidation potential was raised to over $+700$ mV, a small reactive current appeared, and the polypyrrole film began to form on the surface of the platinum electrode and electrons were released by doping. As the potential increased further (up to $+850$ mV), the reactive current increased rapidly. When the potential reached $+850$ mV, the monomer polymerized massively with dopant and gradually increased the thickness of the film. As a result, the massive transfer of electrons to the electrode caused an increase in the reactive current. When the oxidation potential reached $+1000$ mV, the first layer of polypyrrole film was formed on the platinum electrode. The potential cycle was then turned to the 'reduction scan mode'. Reduction curve 1 deviated from oxidation curve 1 with a negative current. This reduction current was produced by the dedoping of anions on the first lamina of the film. A reduction potential of -400 mV was able to sweep most anions through the lamina of film, thus the cathodic current (I_{pc}) appeared. When the reduction potential reached -700 mV, it turned back to the 'oxidation scan mode', which produced the oxidation curve 2. At -100 mV, the anodic current (I_{pa}) was produced as a result of the permeation of the anions in the film toward the solution interface. The appearance of I_{pa} at $+650$ mV was resulted from the massive permeation of anions from the electrolytic solution into the electrode interface of the film. At $+850$ mV, the second lamina of the polypyrrole film was formed. The weaker current at 0 mV

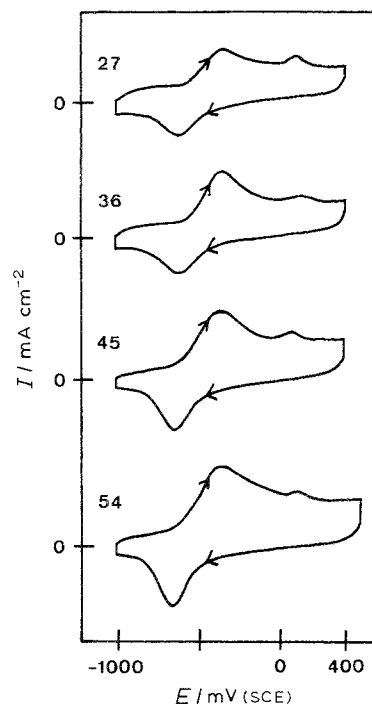


Fig. 2. The relation between pyrrole film's thickness and capacity. Electrolyte solution: 0.1 M; $\text{LiClO}_4 + \text{CH}_3\text{CN}$; scanning rate: 40 mV s^{-1} .

is due to the dedoping of the second lamina of film. In addition, the I_{pc} at -450 mV is the result of dedoping (adverse permeation) of anions on the first lamina and parts of the second lamina. Such repeated scanning of redox potential was able to increase the film thickness and also expand the area of the close curve of the redox reactive current. The thicker the polypyrrole film on the electrode plate, the larger the effective total area for accepting electrons. From these results the redox reactivity of pyrrole may be considered reversible. The anodic current was due to the oxidation during the polymerization of pyrrole with the doping of ClO_4^- into the polypyrrole film matrix. Both anodic and cathodic currents increased with the number of potential cycles, due to the increase of film thickness. These results contradicted the experimental conclusions of Inoue [12].

3.2. Influence of the thickness of polypyrrole films on the redox behaviour

Figure 2 shows the cyclic voltammograms of the redox reaction of polypyrrole films of different thickness in the acetonitrile solution with LiClO_4 . The area of the current-potential curve expanded with the increase of the film thickness. In addition, the expansion of the effective electrode area increased the doping of the anions, thus making the film capacity increase proportionally with the thickness of the film. This phenomenon was contrary to the conclusions of Inoue [12].

The potential difference ($\Delta E_p = E_{pa} - E_{pc}$) is the index of the reversible potential when performing the redox reaction with polypyrrole films. Figure 3 is the E_{pa} , E_{pc} potential diagram of different film thicknesses

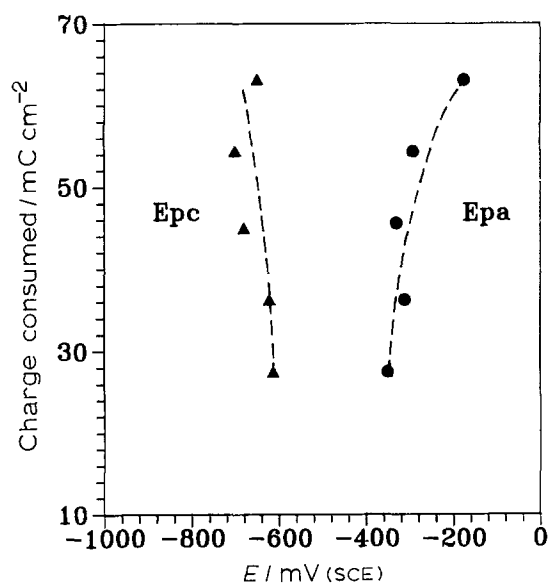


Fig. 3. The location of pyrrole film thickness and E_{pa} , E_{pc} potential. Electrolyte solution: 0.1 M $\text{LiClO}_4 + \text{CH}_3\text{CN}$; scanning rate: 100 mV s^{-1} .

scanned at a rate of 100 mV s^{-1} . E_{pa} increased with the film thickness, while E_{pc} gradually decreased; therefore, ΔE_p increased with the film thickness. This is because the amount of dopant increased with the film thickness, but this hindered further permeation of anions. Higher potential was thus required for the permeation of the doped anions between the lamina of film.

3.3. Effect of the dopant on the redox behaviour of polypyrrole films

To study the effect of the dopant on the redox behaviour of polypyrrole films, samples of the same thickness were immersed in solutions of various electrolytes of different concentrations. Figure 4 is the cyclic voltammogram of the electrochemical reactions in acetonitrile solutions of different concentrations of LiClO_4 . At the same potential, the dopant increased with the ionic concentration, but the area of the

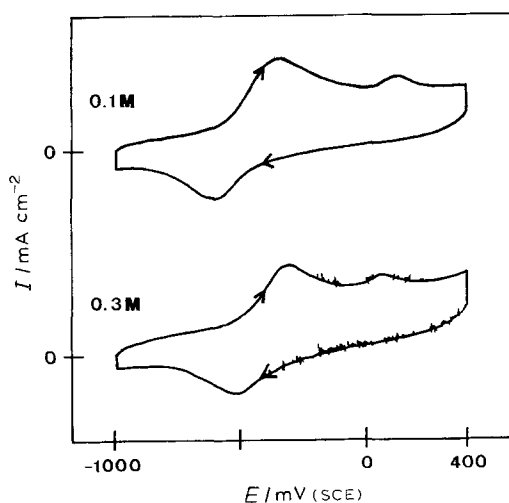


Fig. 4. The cyclic $C-V$ curve of pyrrole film oxidation-reduction reaction in electrolyte solutions of different concentrations. Film polymerizing time: 2 min; electrolyte solution $\text{LiClO}_4 + \text{CH}_3\text{CN}$.

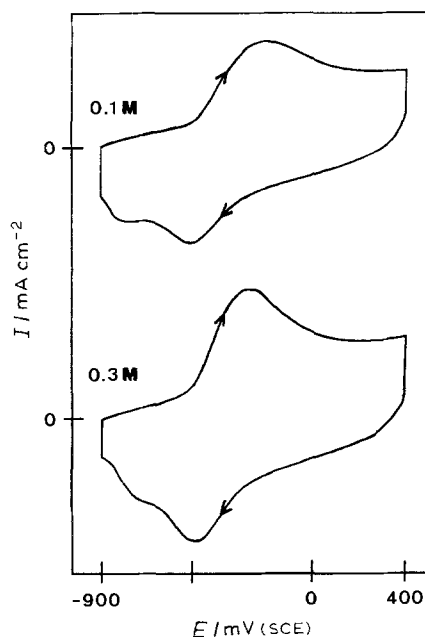


Fig. 5. The cyclic $C-V$ curve of pyrrole film oxidation-reduction reaction in solutions of different concentrations. Film polymerizing time: 2 min; electrolyte solution: $\text{KCl} + \text{H}_2\text{O}$.

current-potential curve did not expand with the electrolyte concentration. This is due to the larger size of ClO_4^- . Although under the potential polarization effect, there was a high concentration of ClO_4^- ions moving to the interface between film and solution, the permeation and thus the amount of doping of ClO_4^- were blocked by the smaller microvoids of the film. Thus the area of the current-potential curve did not expand with the higher concentration of ClO_4^- . In addition, the larger size of ClO_4^- lowered the permeability and thus caused the oscillation in the reactive current.

Figure 5 shows the electrochemical reaction performed in a KCl solution. At equal potential, the solution with higher anionic concentration yielded a current-potential curve of larger area and more doping. Because the size of Cl^- is smaller than ClO_4^- its permeability was not blocked by the microvoids of the lamina and thus the amount of doping increased. Because of the small size of Cl^- , oscillation did not occur in the reactive current.

3.4. Effect of the conductivity of the electrolyte solution on the redox behaviour

According to the results of the experiment, the conductivities of the electrolyte-solution pairs are as follows: $\text{KCl} + \text{H}_2\text{O} > \text{LiClO}_4 + \text{CH}_3\text{CN} > \text{Et}_4\text{NBF}_4 + \text{CH}_3\text{CN} > \text{Et}_4\text{NClO}_4 + \text{CH}_3\text{CN} > \text{Et}_4\text{NCl} + \text{CH}_3\text{CN}$. Figure 6 is the cyclic voltammogram of the redox reaction of polypyrrole films of the same thickness in different electrolyte solutions. At the same electrolyte concentration, both the mobility and permeability of the anion were affected by the conductivity of the solution. The sizes of LiClO_4 , Et_4NClO_4 , and Et_4NBF_4 were almost equal, while KCl was the smallest. Only the electrolyte solutions of LiClO_4 and

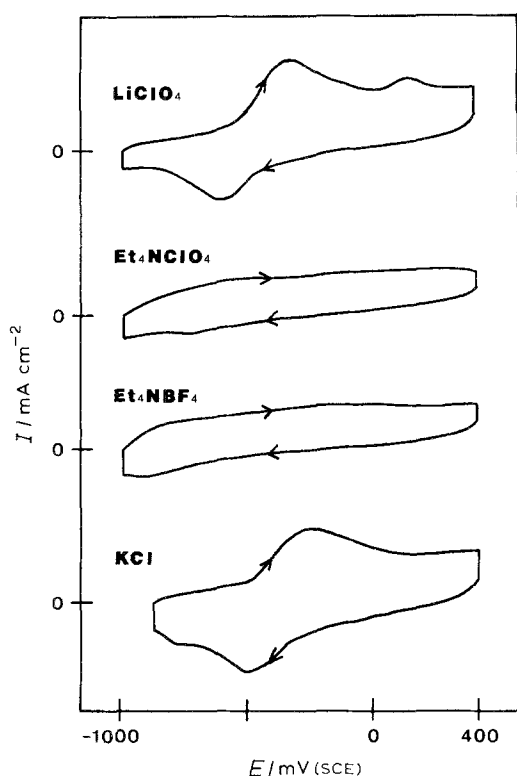


Fig. 6. The cyclic C - V curve of pyrrole film oxidation-reduction reaction in different kinds of electrolyte solutions. Film polymerizing time: 2 min.

KCl had redox properties. In the cases of Et_4NClO_4 and Et_4NBF_4 , their reactive currents gradually increased and decreased with the scanning potential, and the amount of doping was small. Neither I_{pa} nor I_{pc} were observed due to the low mobility and permeability of these two electrolytes.

3.5. Electrochromic properties of polypyrrole films

The changes in the conductive mechanism of the energy level can be explained by the shift in the optical absorption [10]. When polypyrrole switches between conductivity and insulation, its colour may change reversibly. The visible spectrum had different shapes due to the applied redox potential, as shown in Fig. 7. When doping occurred under the oxidation potential, the film was black, and the spectrum curve was smooth. When dedoping occurred under the reduction potential, the film was light yellow, and the spectrum curve peaked near the ultraviolet region.

The spectrum curves of the oxidation and reduction scanning modes form a hysteresis circle of close curve, thus the optical properties of polypyrrole are nonlinear. This behaviour is called a hysteresis of chromism. Figure 8 shows the visible spectra during the electrochemical reaction of polypyrrole films of different thicknesses in an acetonitrile solution of LiClO_4 . The degree of the hysteresis of chromism increased with the film thickness, since the anion permeation was hindered by the thick film. Figure 9 shows the visible spectrum of the redox reaction in an aqueous solution of KCl. Its hysteresis of chromism was not as apparent as in Fig. 8. This spectrum was more similar to linear optics, and the

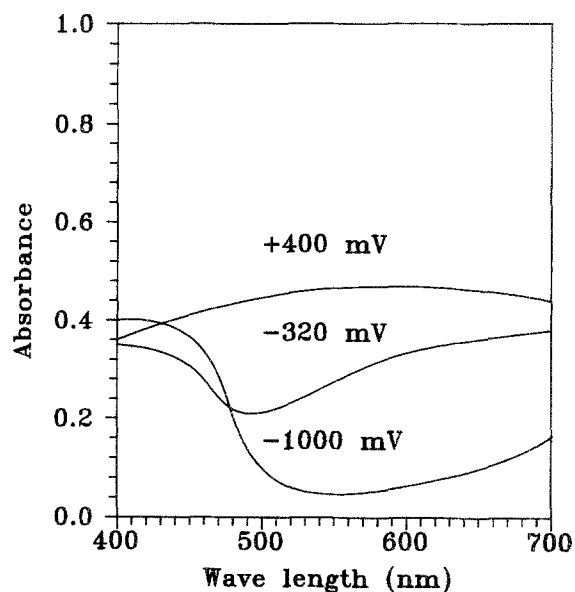


Fig. 7. The relation between pyrrole film visible spectrum absorption factor and given potential. Film polymerizing time: 2 min; electrolyte solution: 0.1 M $\text{LiClO}_4 + \text{CH}_3\text{CN}$; scanning rate: 20 mV s^{-1} .

rate of colour change was much higher. Here the anion has higher permeability due to the smaller size of Cl^- and better conductivity of the solution.

The difference in the corresponding spectra between the initial oxidation potential and the final reduction potential, as shown in Fig. 9, is called the hysteresis index (Δ_{abs}). The smaller Δ_{abs} is the more technicoloured, in other words, the more vivid the colour change. As shown in Fig. 8, the thicker film had a larger Δ_{abs} , thus it was not technicoloured in the process of chromism. This behaviour was also influenced by the anion permeability. As shown in Fig. 10, films in the KCl solution had the smallest Δ_{abs} . Because of the better conductivity of the solution and the smaller anion size,

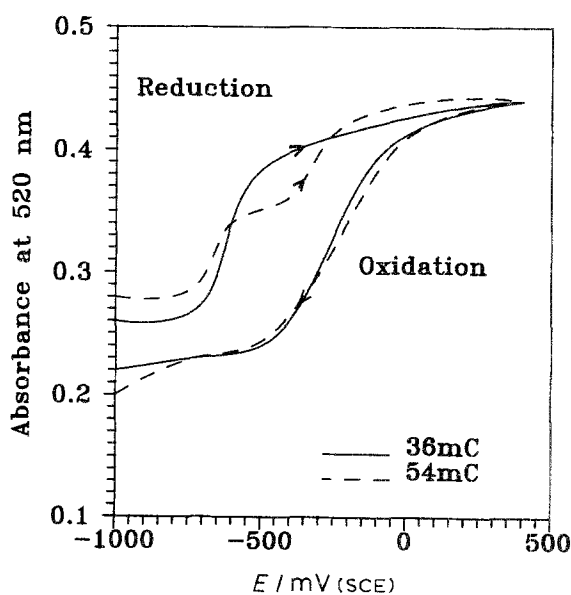


Fig. 8. The hysteresis relation between pyrrole film thickness and the change in the spectrum absorption factor in its oxidation, reduction reaction. Electrolyte solution: 0.1 M $\text{LiClO}_4 + \text{CH}_3\text{CN}$; scanning rate: 20 mV s^{-1} .

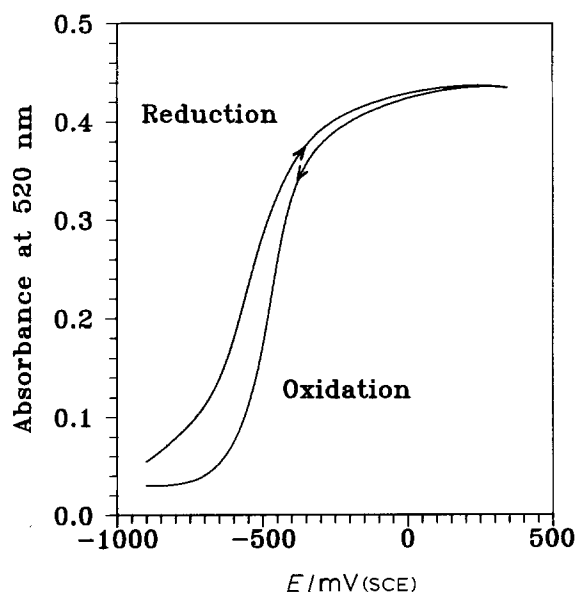


Fig. 9. The hysteresis relation between pyrrole film oxidation and reduction in solutions and the change in the spectrum absorption factor. Film polymerizing time: 2 min; electrolyte solution: 0.1 M KCl + H₂O; scanning rate: 20 mV s⁻¹.

the dopant permeability was higher. As a result, polypyrrole in a KCl aqueous solution had the most vivid change of colour and was the most technicoloured.

3.6. Response time of the electrochromic reaction for polypyrrole films by pulse function

The square wave applied to the electrochemical system had an amplitude of 900 mV and a duration of 6 s, as shown in Fig. 11. Also shown are the charging and discharging reactions of polypyrrole films of different thicknesses in the 0.1 M acetonitrile solution of LiClO₄. At the instant of charging, due to the polarization of the potential, massive ClO₄⁻ permeated the film lamina. The reactive current jumped immediately. But the lamina structure was unable to accommodate all the permeated dopants, thus after the instant of charging, the current rapidly decreased and then faded away. As indicated by the charging response times,

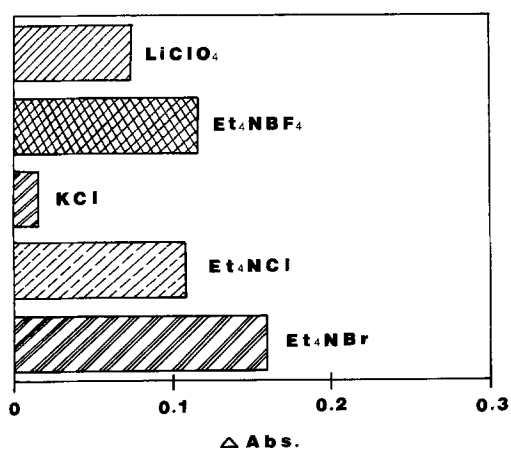


Fig. 10. The hysteresis relation between pyrrole film oxidation and reduction reactions in different kinds of electrolyte solutions, and the change in the spectrum absorption factor. Film polymerizing time; 2 min; scanning rate: 20 mV s⁻¹.

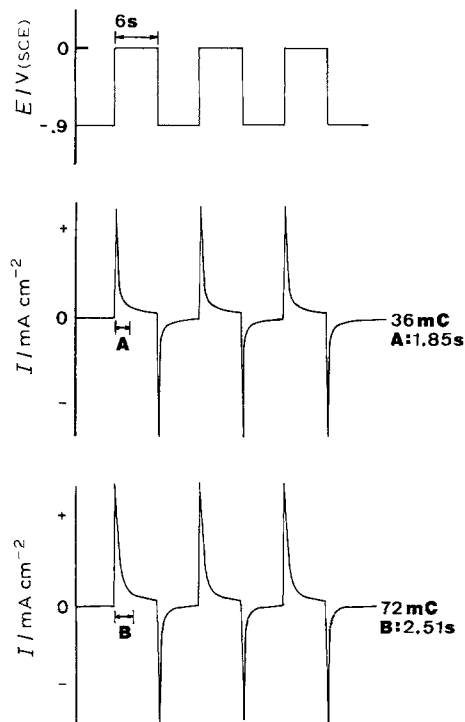


Fig. 11. The relation between pyrrole film thickness and response time. Electrolyte solution: 0.1 M LiClO₄ + CH₃CN.

$A = 1.85$ s, $B = 2.51$ s, the thinner film had a higher rate of anion permeation as well as a higher rate of response. The charging and discharging responses of different electrolytes, as shown in Fig. 12, indicated that the films in the aqueous solution of KCl had a faster response than those in the acetonitrile solution

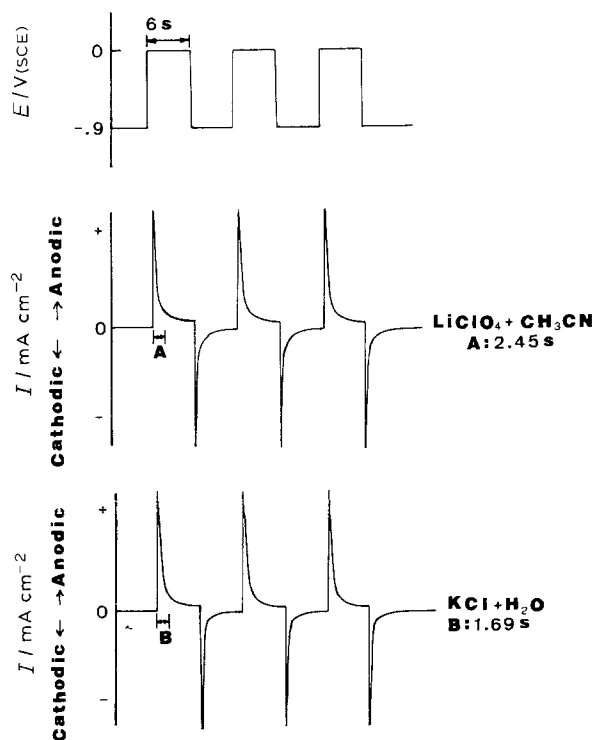


Fig. 12. The response time of polypyrrole film with various electrolyte solutions. Film polymerizing time: 3 min.

of LiClO_4 . Thus for equal film thickness, better conductivity of solution and smaller anion size may facilitate the dopant permeation.

4. Conclusion

In the electrochemical polymerization of pyrrole, the area of the current-potential curve for the redox reaction increases with the film thickness. The increase of film thickness may block the permeation of anions and hence increase the reversible potential. This would affect the driving voltage in making devices. In addition, smaller anions have higher permeability, and thus increase the amount of doping and hence the conductivity of polypyrrole films. Redox reactions may occur only in those electrolyte solutions with high conductivity.

The optical linearity in the spectrum curve of polypyrrole is affected by the amount and the permeability of the dopants. With smaller anions and better conductivity of the solution, the film shows more technical colour in the process of colour change. In order to accelerate the response rate of electrochromism, the film thickness must be decreased, the dopant should have the smallest anion, and the solutions should have high conductivity. Thus the KCl aqueous solution would provide the most vivid electrochromic properties and the fastest response.

Acknowledgement

We thank the National Science Council of the Republic of China for the support of this work under the project NSC 78-0405-E011-08.

References

- [1] A. F. Diaz and K. K. Kanazawa, *J. Chem. Soc., Chem. Commun.* (1979) 635.
- [2] A. F. Diaz and J. I. Castillo, *ibid.* (1980) 397.
- [3] A. F. Diaz, J. I. Castillo, J. A. Logan and Wen-Young Lee, *J. Electroanal. Chem.* **129** (1981) 115.
- [4] A. F. Diaz, A. Martinez and K. K. Kanazawa, *ibid.* **130** (1981) 181.
- [5] A. F. Diaz, K. K. Kanazawa, J. I. Castillo, and J. A. Logan, *Polym. Sci. Tech.* **15** (1981) 149.
- [6] S. Kuwabata, H. Yoneyama, and H. Tamura, *Bull. Chem. Soc. Jpn.* **57** (1984) 2247.
- [7] K. Kaneto, K. Yoshino and Y. Inuishi, *Jpn. J. Appl. Phys.* **22** (1983) L412.
- [8] R. J. Waltman, A. F. Diaz and J. Bargon, *J. Electroanal. Soc.* **131** (1984) 1452.
- [9] C. R. Fincher, Jr., M. Ozaki, A. J. Heeger and A. G. MacDiarmid, *Phys. Rev. B.* **19** (1979) 4140.
- [10] C. R. Fincher, Jr., M. Ozaki, M. Tanaka, D. Peebles, L. Lauchlan, A. J. Heeger and A. G. MacDiarmid, *ibid.* **20** (1979) 1589.
- [11] E. K. Sichel, M. F. Rubner and S. K. Tripathy, *ibid.* **26** (1982) 6719.
- [12] T. Inoue and T. Yamase, *Bull. Chem. Soc. Jpn.* **56** (1983) 985.